07

Light-emitting diodes based on GaInAsSb solid solutions for the spectral range of 2.5−2.8 μm

© Ya.A. Parkhomenko, E.V. Ivanov, E.V. Kunitsyna, A.A. Pivovarova, A.V. Nashchekin, I.A. Andreev, N.D. Il'inskaya, Yu.P. Yakovlev

Ioffe Institute, St. Petersburg, Russia
E-mail: Ed@mail.ioffe.ru

Received June 27, 2025
Revised August 1, 2025
Accepted August 2, 2025

For the first time LEDs emitting in the wavelength range of 2.5−2.8 μm at room temperature were created on the base of *n*-GaSb/*n*-$Ga_{0.74}In_{0.26}As_{0.22}Sb_{0.78}$/*p*-GaSb heterostructures grown by liquid-phase epitaxy using lead as a neutral solvent. The results of the study of electrical and electroluminescent characteristics for these LEDs are presented. In quasi-CW mode at the injection current of 200 mA the pulse optical power was equal to 7.4 μW. The developed LEDs are able to be used for detection of carbon dioxide and water vapor in the atmosphere.

Keywords: light-emitting diodes, electroluminescence, GaSb/GaInAsSb heterostructures, liquid-phase epitaxy, lead-containing solutions-melts.

DOI: 10.61011/TPL.2025.11.62201.20419

The spectral range of 2−5 μm contains several fundamental absorption bands of carbon dioxide (CO_2) [1], which is the main greenhouse gas and may be harmful to humans [2]. When CO_2 is detected by the optical absorption method, the most intense band located at wavelength $\lambda = 4.3\,\mu$m is typically used [3,4]. At the same time, carbon dioxide has another strong absorption band in the region of 2.7−2.8 μm, and the optical power of LEDs emitting within the two-micron wavelength range exceeds significantly the power level of LEDs operating in the region of 4−5 μm [5]. However, the absorption bands of CO_2 in the vicinity of 2.70 and 2.77 μm overlap with intense absorption bands of water vapor ($\lambda \approx 2.68$ and 2.78 μm) [1], which makes it somewhat difficult to use them [6–8]. Nevertheless, the presence of an absorption band associated exclusively with water molecules at wavelength $\lambda \approx 2.60\,\mu$m makes it possible to distinguish between the influences of CO_2 and H_2O and detect these substances separately.

We have already studied the electrical and electroluminescent (EL) characteristics of LEDs with a spectral maximum around 2.3 and 2.44 μm, in the active regions of which $Ga_{1-x}In_xAsSb$ ($x = 0.21$ and 0.25, respectively) solid solutions grown by liquid-phase epitaxy (LPE) from lead-containing solutions-melts were used [9]. The presence of lead in the liquid phase makes it possible to alter the boundary of the miscibility gap and ensure an indium content of more than 0.24 in $Ga_{1-x}In_xAsSb$ solid solutions obtained at temperature $T = 560\,^\circ$C.

The present work is a continuation of earlier studies that is aimed at advancing further into the long-wavelength EL region for the detection of CO_2 in the absorption band near 2.7 μm. Isoperiodic $Ga_{1-x}In_xAsSb$ solid solutions with indium content $x > 0.25$ are needed to solve this problem. The only way to obtain such materials without lowering significantly the epitaxy temperature is to use a neutral solvent.

The *n*-GaSb/*n*-GaInAsSb/*p*-GaSb heterostructures have been grown by LPE on *n*-GaSb:Te (100) substrates with the carrier concentration $n = (1-5)\cdot 10^{17}\,\mathrm{cm}^{-3}$. A $Ga_{0.74}In_{0.26}As_{0.22}Sb_{0.78}$ layer with thickness $d \sim 0.15\,\mu$m grown from lead-containing solutions-melts was the active region. The band gap of the $Ga_{0.74}In_{0.26}As_{0.22}Sb_{0.78}$ solid solution was calculated based on the bowing parameters for the quasi-binary system [10] to be $E_g = 0.47-0.49$ eV (at $T = 300$ K). The *p*-GaSb:Ge cap layer with a thickness of 2.5 μm was a wide-gap emitter. In the process of epitaxy, the GaInAsSb solid solution was doped with Te. Two types of heterostructures differing in carrier concentration n in the active region were grown this way: structures *A* ($n \sim 3\cdot 10^{17}\,\mathrm{cm}^{-3}$) and *B* ($n \sim 5\cdot 10^{16}\,\mathrm{cm}^{-3}$). According to X-ray diffractometry data, the mismatch between the crystal lattice periods of epitaxial layers and the substrate was no more than $1\cdot 10^{-3}$. The chemical composition of quaternary solid solution $Ga_{1-x}In_xAs_ySb_{1-y}$ was determined by quantitative X-ray spectral analysis using a JXA-5 CAMEBAX microanalyzer.

Ring contacts of LED chips (width, 30 μm; inner diameter, 200 μm) and a square mesa 400 × 400 μm in size were formed by contact photolithography and wet chemical etching from the side of the top *p*-GaSb layer. Ohmic contacts to *n*- and *p*-type materials were formed by high-vacuum thermal sputtering of the Cr−Au−Ni−Au system with subsequent annealing in a hydrogen atmosphere. The ring ohmic contact thickness was increased to ∼ 2 μm by local electrochemical deposition of Au. The Cr−Au system was sputtered additionally from the *n*-GaSb substrate side onto the solid ohmic contact to a total thickness of ∼ 0.6 μm. LED chips were mounted on TO-18 packages with the substrate facing the base.

The current–voltage (I−V) curves and EL characteristics of LEDs based on *n*-GaSb/*n*-GaInAsSb/*p*-GaSb heterostruc-

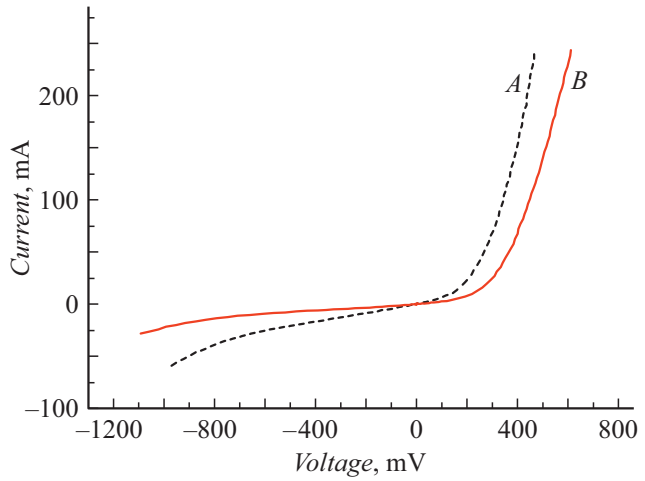

Figure 1. Current–voltage curves of heterostructures *A* and *B* at temperature $T = 300$ K.

tures were examined at room temperature. An automated setup connected to a personal computer was used to record the I–V curves. The so-called quasi-CW supply mode was implemented in experiments with the studied structures: rectangular current pulses with a duty factor of 50 % and a repetition rate of 512 Hz. In the case of forward bias, the negative potential was applied to the *n*-GaSb substrate and the positive one was applied to the *p*-GaSb cap layer; reverse bias corresponded to the opposite polarity.

The spectral characteristics of EL were studied using an automated setup based on a DK-480 monochromator (CVI Laser Corp., NM) with a 300 mm^{-1} diffraction grating, a J10D-M204-R04M-60 InSb photovoltaic detector (Judson Technologies, PA) cooled with liquid nitrogen, and an SR-810 digital lock-in amplifier (Stanford Research Systems Inc., CA). The monochromator, photodetector, and other measuring instruments were calibrated by the manufacturers under workshop conditions. Optical radiation emerging from the heterostructure through the top *p*-GaSb layer was recorded. The measured and digitized photo signal was transmitted to a computer that controlled the process of spectra measurement. EL was excited in the forward bias mode by rectangular current pulses with the same characteristics as those set for I–V measurement.

A calibrated J10D-M204-R04M-60 photodetector was used to determine the absolute values of optical power. The power EL characteristics of LEDs were determined taking into account the radiation pattern.

Typical I–V curves recorded for heterostructures *A* and *B* are shown in Fig. 1. The examined heterostructures had a diode dependence of current on applied voltage. The forward branch of I–V curve for the structure *B* was characterized by higher values of turn-on voltage $U_0 \approx 0.32–0.38$ V (for different samples) and series resistance $R_S \approx 0.8–1.2\,\Omega$ than that of structure *A* ($U_0 \approx 0.25–0.28$ V, $R_S \approx 0.8–0.9\,\Omega$). The ratio of series resistance values is consistent with the data on the carrier concentration in GaInAsSb active layer for heterostructures *A* and *B*. At the same time, the measured turn-on voltage values for both structures were noticeably smaller than the band gap of the $Ga_{0.74}In_{0.26}As_{0.22}Sb_{0.78}$ active region ($E_g \approx 0.48$ eV).

A similar ratio between parameters U_0 and E_g was observed earlier in the study of LEDs based on InAs/InAsSb/InAsSbP heterostructures with an EL maximum in the region of 4.3 and 4.7 μm [4]. Apparently, the low values of U_0 are attributable to leakage currents through dopant-induced levels in the bulk of heterostructures. Large magnitudes of current in the reverse branch of I–V dependences (Fig. 1) support this explanation. In addition, the indicated currents for heterostructure *A* were higher in absolute value than those corresponding to structure *B*, which was characterized by a lower concentration of the dopant in the active region ($I \approx -50$ and -20 mA at $U = -0.8$ V, respectively).

Figure 2 shows the EL spectra for heterostructures *A* and *B* measured at different injection current magnitudes. The EL spectra of the studied structures differed in intensity, while the other parameters (position of the maximum, shape, and width at half maximum of the spectrum) remained the same. Each EL spectrum is a single band containing several characteristic dips of varying depth and current-independent shape and position. These dips are associated with the absorption bands of water and carbon dioxide molecules present in air [1].

It can be seen from the figure that the shape of EL spectra of each heterostructure, their width at half maximum, and the position of the maximum remained almost unchanged within the entire range of injection currents from 50 to 200 mA. The maximum of the EL spectra is found at wavelength $\lambda_{max} = 2.52$ μm, and the width at half maximum is $\Delta\lambda \approx 420$ nm. In units of photon energy, these values correspond to $h\nu_{max} = 0.49$ eV and $\Delta(h\nu) \approx 80$ meV $\sim 3kT$, where k is the Boltzmann constant. Absorption bands

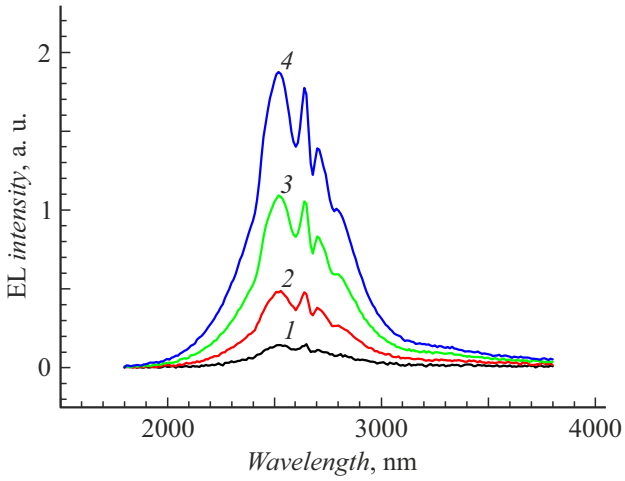

Figure 2. EL spectra recorded for heterostructures *A* and *B* at $T = 300$ K at different injection currents. *I*, mA: *1* — 50, *2* — 100, *3* — 150, *4* — 200.

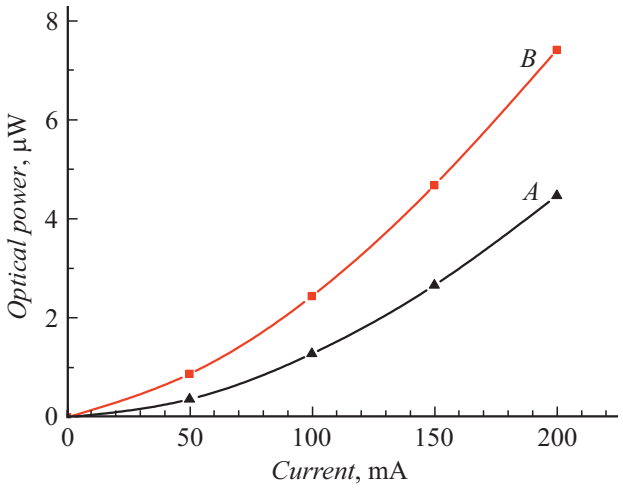

Figure 3. Current dependences of pulse optical power for heterostructures A and B at temperature $T = 300$ K.

increase the width of the EL spectra and alter their shape and the position of the maximum. We assume that the wavelength at the maximum determined with zero absorption should have a slightly larger value than the one following from Fig. 2. According to our estimates, the actual value is $\lambda_{max} \approx 2.6\,\mu$m, which is consistent with the band gap of solid solution $Ga_{0.74}In_{0.26}As_{0.22}Sb_{0.78}$. The measurement of EL characteristics undistorted by the absorption bands of H_2O and CO_2 will be the subject of further research.

Characteristic dependences of pulse optical power P on injection current I for LEDs fabricated on the basis of heterostructures A and B are shown in Fig. 3. Both curves are approximated well by a power superlinear function $P \propto I^M$, where $M > 1$. The EL power for the studied heterostructures is several microwatts, which is significantly lower than the characteristic power levels of LEDs operating within the two-micrometer wavelength range [5,9]. It should be noted that the nonlinear dependence of power on current for heterostructure B is less pronounced ($M \approx 1.5-1.6$) than in structure A ($M \approx 1.8-1.9$). At the same time, heterostructure B provides a higher optical power level (different samples have $P \approx 1.8-4.7\,\mu$W at $I = 150$ mA) than structure A ($P \approx 1.4-2.6\,\mu$W at the same current). The external quantum efficiency for the studied structures does not exceed $0.75 \cdot 10^{-2}$ % (Fig. 3, curve B: $P \approx 7.4\,\mu$W at $I = 200$ mA). The corresponding internal quantum efficiency is ~ 0.66 %. These features suggest that the superlinear $P(I)$ dependence is formed under the influence of nonradiative Shockley–Read–Hall recombination at crystalline defects in the active region of heterostructures [11].

Apparently, the main reason for the low efficiency of radiative recombination is the small thickness of $Ga_{0.74}In_{0.26}As_{0.22}Sb_{0.78}$ active layer ($d \sim 0.15\,\mu$m). In turn, small values of d are attributable to technological difficulties of growth near the boundaries of the miscibility gap. Overcoming these problems is an objective of future research.

We have already fabricated LEDs based on InAs/InAsSbP heterostructures that emitted at room temperature within the spectral range of $2.6-2.8\,\mu$m [12]. At a current of 200 mA in the quasi-CW mode, the output optical power of these LEDs was $\sim 1.8-2.3\,\mu$W. These parameters are several times lower than the corresponding power values for heterostructures A and B presented above.

Thus, GaSb/$Ga_{1-x}In_xAsSb$ ($x = 0.26$) heterostructures have been grown for the first time by LPE from solutions-melts containing lead as a neutral solvent. LEDs with the EL maximum within the range of $2.5-2.7\,\mu$m (at $T = 300$ K) were designed based on them. The results of experiments suggest that these LEDs may find application in various optoelectronic systems as compact and efficient radiation sources for detecting carbon dioxide and humidity in air.

Conflict of interest

The authors declare that they have no conflict of interest.

References

[1] G.G. Ishanin, E.D. Pankov, A.L. Andreev, G.V. Pol'shchikov, *Istochniki i priemniki izlucheniya* (Politekhnika, SPb., 1991), pp. 48–52 (in Russian).
[2] I.I. Novikova, A.V. Sorokina, M.A. Lobkis, N.A. Zubtsovskaya, M.V. Semenikhina, V.A. Shcheveleva, N.I. Nazimkin, Ross. Vestn. Gig., No. 4, 18 (2023) (in Russian). DOI: 10.24075/rbh.2023.081
[3] J.G. Growder, S.D. Smith, A. Vass, J. Keddie, in *Mid-infrared Semiconductor Optoelectronics*, ed. by A. Krier. Springer Ser. in Optical Sciences (Springer-Verlag, London, 2006), p. 595–597.
[4] V.V. Romanov, I.A. Belykh, E.V. Ivanov, P.A. Alekseev, N.D. Il'inskaya, Yu.P. Yakovlev, Semiconductors, **53** (6), 822 (2019). DOI: 10.1134/S1063782619060174.
[5] http://www.ibsg.ru
[6] M.M. Kugeiko, A.A. Baravik, J. Phys.: Conf. Ser., **2127**, 012042 (2021). DOI: 10.1088/1742-6596/2127/1/012042
[7] V.M. Deichuli, T.M. Petrova, A.A. Solodov, A.M. Solodov, Atmos. Ocean. Opt., **35** (6), 634 (2022). DOI: 10.1134/S1024856022060070.
[8] É. Ducreux, B. Grouiez, S. Robert, M. Lepére, B. Vispoel, R.R. Gamache, L. Régalia, J. Quant. Spectrosc. Radiat. Transfer, **323**, 109026 (2024). DOI: 10.1016/j.jqsrt.2024.109026
[9] A.P. Astakhova, E.A. Grebenshchikova, E.V. Ivanov, A.N. Imenkov, E.V. Kunitsyna, Ya.A. Parkhomenko, Yu.P. Yakovlev, Semiconductors, **38** (12), 1419 (2004). DOI: 10.1134/1.1836064].
[10] J.C. DeWinter, M.A. Pollack, A.K. Sritastava, J.L. Zyskind, J. Electron. Mater., **14** (6), 729 (1985). DOI: 10.1007/BF02654308
[11] A.E. Zhukov. *Osnovy fiziki i tekhnologii poluprovodnikovykh lazerov* (Izd. Akad. Univ., SPb., 2016), Vol. 4, pp. 27–32 (in Russian).
[12] V.V. Romanov, E.V. Ivanov, A.N. Imenkov, N.M. Kolchanova, K.D. Moiseev, N.D. Stoyanov, Yu.P. Yakovlev, Tech. Phys. Lett., **27** (7), 611 (2001). DOI: 10.1134/1.1388961.

Translated by D.Safin